

# Near-infrared Shielding and Far-infrared Emission Textiles Coated by Self-assembly Cs<sub>0.32</sub>WO<sub>3</sub> Nanosheets

Linghui Peng, Weifan Chen, Aibing Yu, and Xuchuan Jiang

**Abstract**—Near infrared (NIR) shielding textiles have attracted a great interest recently for energy saving and human comfort. On the other hand, far infrared (FIR) rays with a longer wavelength of 6-15 μm can enhance blood microcirculation and metabolism. Therefore, FIR emission fabric also shows commercial value. Self-assembly Cs<sub>0.32</sub>WO<sub>3</sub> nanosheets coated textile can achieve NIR shielding and FIR emission functions at the same time by applying single functional material--Cs<sub>0.32</sub>WO<sub>3</sub> nanosheets to cotton fibers. Cs<sub>0.32</sub>WO<sub>3</sub> is known as a great NIR absorber and it is also a far infrared emitter. NIR is absorbed by Cs<sub>0.32</sub>WO<sub>3</sub> nanosheets and converted into FIR radiation for human blood circulation. Compared with current infrared shielding textiles using solid-liquid phase change materials (PCMs), Cs<sub>0.32</sub>WO<sub>3</sub> coated textiles possess better shielding property and longer service life, no leakage and FIR emission. The excellent NIR absorber Cs<sub>0.32</sub>WO<sub>3</sub> nanosheets were successfully synthesized in this study. The coated fabrics were tested for NIR shielding property, FIR emissivity and laundering durability. Cs<sub>0.32</sub>WO<sub>3</sub> coated textiles with excellent infrared shielding performance of lowering the temperature of about 4.5 °C, good FIR emissivity of increasing fabric surface temperature to 64 °C, and washing durability were comprehensively maintained.

**Index Terms**—Infrared shielding, infrared emission, functional fabric, Cs<sub>0.32</sub>WO<sub>3</sub>.

## I. INTRODUCTION

The main functions of the traditional textiles were to keep the human body warm and dry in cold climates and to protect human from the heat and sun in hot climates. Today, continuous growth in the world's population and improvements in living standards have required textiles with new functions to meet changing needs. Thermal physiological comfort is important for apparels when there are challenging temperature conditions [1]. Outdoor thermal comfort can not be achieved by air conditioning like indoor. Without air conditioning, clothing becomes the important way to control human body temperature. However, common clothing has limited range of thermal insulation and solar blocking, which often fails to shield solar radiation from sun in hot summer.

Sunlight that reaches the human skin contains solar

energy composed of 5% ultraviolet (UV), 50% visible light and 45% infrared radiation as shown in Fig. 1 (a). Long time UV exposure on human skin can cause skin cancer, which has been proven by many studies [2]. UV blocking textiles have been studied for many years. TiO<sub>2</sub>, silver, ZnO and so on have been applied to the textile for UV blocking [3], [4]. However, human skin is actually exposed to tremendous amounts of natural near-infrared (NIR) from the sun as well, especially people in outdoors. In reality, NIR can penetrate the skin, which may induce photoaging and potentially photocarcinogenesis [5]. Few studies investigate NIR shielding recently. Some materials, including hollow microspheres [6], silver [7] and TiO<sub>2</sub>/SiO<sub>2</sub> [8], can be applied on the surface of the fabric to reflect the NIR for shielding. However, the reflection rate of this kind of textile is relatively low due to disconnection between fibers and rough surface of the fabric. Therefore, the necessity of high efficiency solar NIR shielding textile should be considered.

On the other hand, far-infrared (FIR) rays with a longer wavelength of 6-15 μm can penetrate 2-3 mm [9] into skins and exert strong rotational and vibrational effects at the molecular level, leading to dilation of blood vessels and therefore, enhancement of blood microcirculation and metabolism [10]. FIR emitting materials would transform the energy absorbed from either sunlight or heat of the human body into FIR rays within a specific wavelength range, and then reemit them to the human body [11]. Because FIR radiation enhances blood circulation and metabolism as well as promotes the recovery of fatigued muscles [12], much attention has been paid to the application of far infrared emission materials to textiles that have close contact with the skin for therapeutic and health care purposes [13], [14].

Cesium-doped tungsten oxide Cs<sub>0.32</sub>WO<sub>3</sub> is an ideal NIR shielding material for solar control [15]. Thin films prepared with these nanoparticles even at a low percentage (0.2 wt%) can reach a high NIR shielding efficiency in the whole wave range of NIR. Cs<sub>0.32</sub>WO<sub>3</sub> nanoparticles possess good chemical stability and non-toxic, which are suitable for textile applications. However, there is only one research that applied Cs<sub>0.32</sub>WO<sub>3</sub> to textiles for IR blocking [16], and far IR emission of the coated textile has not been investigated.

In this study, Cs<sub>0.32</sub>WO<sub>3</sub> nanosheets were synthesized through a scalable mechanochemical synthesis method accompanied by a mechanical bead-mill process, which is waterless and environmental friendly. As synthesized Cs<sub>0.32</sub>WO<sub>3</sub> nanosheets were characterized by transmission electron microscopy (TEM), scanning electron microscopy (SEM) and X-ray diffraction (XRD). Cs<sub>0.32</sub>WO<sub>3</sub> nanosheets were self-assembled on cotton fabric with assistance of

Manuscript received July 12, 2019; revised August 29, 2019.

Linghui Peng, Aibing Yu, and Xuchuan Jiang are with Department of Chemical Engineering, Monash University, Australia (linghui.peng@monash.edu, Xuchuan.Jiang@monash.edu, aibing.yu@monash.edu).

Weifan Chen is with School of Materials Science and Engineering, Nanchang University, China (weifan-chen@163.com).

PDDA (as shown in Fig. 1 (b)) to improve NIR shielding performance in the wave range of 780 to 2600 nm and FIR emission property.  $\text{Cs}_{0.32}\text{WO}_3$  nanosheets coated cotton fabric with excellent NIR shielding properties and FIR emission was prepared FIR as shown in Fig. 1(c). The  $\text{Cs}_{0.32}\text{WO}_3$  nanosheets coated cotton fabrics were characterized by scanning electron microscopy (SEM), Attenuated Total Reflectance infrared spectroscopy (ATR) and atomic force microscopy (AFM). Color characteristics, NIR shielding property and surface temperature under solar radiation of the coated cotton fabrics were evaluated. In addition, the color fastness to washing was employed to evaluate the adhesive strength of the  $\text{Cs}_{0.32}\text{WO}_3$  nanosheets on the cotton fabric modified with Poly(diallyldimethyl ammonium chloride) (PDDA).  $\text{Cs}_{0.32}\text{WO}_3$  nanosheets coated cotton fabrics can achieve NIR shielding, FIR emission multifunctions within a fabric by only using  $\text{Cs}_{0.32}\text{WO}_3$  nanosheets as functional materials. This kind of fabric can be used in outdoor NIR shielding, photo-thermal therapy for health care and other related areas.

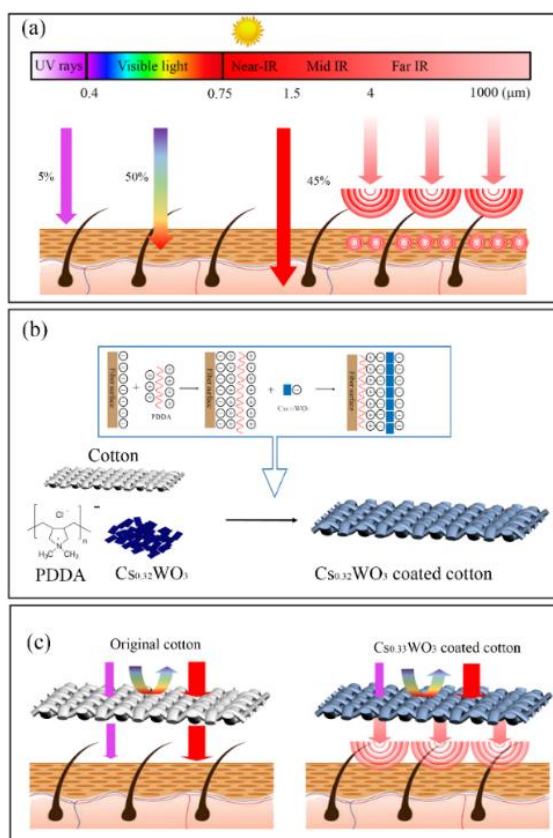


Fig.1. (a) Solar radiation on the skin, (b) Schematic of fabricating of  $\text{Cs}_{0.32}\text{WO}_3$  nanosheets coated textiles and (c)  $\text{Cs}_{0.32}\text{WO}_3$  nanosheets coated textiles for near IR shielding and far IR emission.

## II. METHOD

### A. Materials

100% Cotton fabric ( $84.0\text{g}/\text{m}^2$ ) was purchased from spotlight. 20 wt% Poly(diallyldimethylammonium chloride) (PDDA) was purchased from Sigma. Sodium tungstate dihydrate ( $\text{Na}_2\text{WO}_4 \cdot 2\text{H}_2\text{O}$ ), oxalate dihydrate ( $\text{H}_2\text{C}_2\text{O}_4 \cdot 2\text{H}_2\text{O}$ ), and dehydrated ethanol were of analytical grade, used without further purification, and purchased from Damao chemical reagent factory. All of the chemicals were used as received.

### B. Preparation of $\text{Cs}_{0.32}\text{WO}_3$ Nanosheets

$\text{Cs}_{0.32}\text{WO}_3$  nanosheets were synthesized based on our previous work [17]. In a typical experiment, 32.95 g of  $\text{Na}_2\text{WO}_4 \cdot 2\text{H}_2\text{O}$  (0.10 mol) and 12.73 g of  $\text{H}_2\text{C}_2\text{O}_4 \cdot 2\text{H}_2\text{O}$  (0.10 mol) were placed into Teflon ball milling pots of 500 mL that loaded with 280 g of zirconia milling balls of 8 mm in diameter. Then they were transferred to a three-dimensional rotary planetary ball mill for milling at 1800 rpm for the designed period. Next, the as milled pasty powders were washed successively by using deionized water and dehydrated ethanol several times. Followed by drying in a blast air oven at  $60^\circ\text{C}$  for 2 h, about 24.30 g of  $\text{WO}_3 \cdot 2\text{H}_2\text{O}$  ultrathin narrow nanosheets can be obtained. The as-prepared  $\text{WO}_3 \cdot 2\text{H}_2\text{O}$  nanosheets and  $\text{Cs}_2\text{CO}_3$  were ground at 1800 rpm for 60 min using a planetary ball mill. After the as-milled mixtures were calcined in a tube furnace set at  $500^\circ\text{C}$  for 120 min under a flowing  $\text{H}_2/\text{N}_2$  gas mixture ( $\text{H}_2/\text{N}_2 = 5/95$  in volume). Finally,  $\text{Cs}_{0.32}\text{WO}_3$  nanosheets were obtained.

### C. Fabrication of Near Infrared Shielding Textile

Cotton fabrics ( $8\text{cm} \times 8\text{cm}$ ) were firstly washed by ethanol and acetone in the ultrasonic bath for 30 min respectively. Then they were washed with flowing deionized water for 5 min and dry in oven at  $60^\circ\text{C}$  for 2 h. Cotton fabrics were dipped into 10g/L of 20 % PDDA solution (200 ml) for 24 h, and then they were washed by deionized water and dried at  $60^\circ\text{C}$  in oven.

0.4 g  $\text{Cs}_{0.32}\text{WO}_3$  nanosheets were dispersed in 400 mL deionized water at and put into ultrasonic bath for 30 min. The PDDA treated cotton fabric was put into  $\text{Cs}_{0.32}\text{WO}_3$  nanosheets dispersion for 48 h and then washed by deionized water and dried at  $60^\circ\text{C}$  in oven for 5 h.

### D. Characterizations

The microstructure and crystal lattice of the samples were analyzed using a transmission electron microscope (TEM, FEI Tecnai T20, America). The microscopic morphology was obtained using a field-emission scanning electron microscope (FE-SEM, FEI Nova 450, America) with an energy-dispersive spectrometer (EDS) attachment at an acceleration voltage of 5 kV. Surface topography of coated cotton fiber characterized by AFM (Dimension iCon AFM).

X-ray diffraction (XRD) analyses were conducted on a Rigaku Mini flex 600 diffractometer (Japan) with  $\text{Cu K}\alpha$  radiation ( $\lambda = 1.5418 \text{ \AA}$ ) using a voltage and current of 40 kV and 15 mA, respectively. The sample was measured at a scanning rate of  $5^\circ/\text{min}$ .

The pictures of the original and  $\text{Cs}_{0.32}\text{WO}_3$  coated fabrics were taken by a digital camera.

Simulation test: We also characterized the thermal management of the  $\text{Cs}_{0.32}\text{WO}_3$  coated textiles by using a system which simulated the real environment. A box ( $18 \times 18 \times 10 \text{ cm}^3$ ) with a  $6 \times 6 \text{ cm}$  window was made of 0.5 cm thick glass covered by aluminum foil paper for insulation. The fabric samples were placed onto the top window of the box. One identical infrared lamp (PHILIPS, R125 IR R 150 W, Shanghai) was used as heat sources and kept at 40 cm distance to simulate solar radiation. The surface temperatures of the samples were detected by infrared camera by Fluke TIS45 Thermal Imaging Camera.

A model house test is used to clearly demonstrate the NIR shielding performance of the  $\text{Cs}_{0.32}\text{WO}_3$  nanosheets coated fabric for a practical application. A model house was made of 1.5 cm thick planks. These planks were painted on both sides for thermal insulation. The treated textile and untreated textile were pasted onto the front of the room ( $25 \times 30 \text{ cm}^2$ ). Two identical infrared lamps were used as heat sources to simulate solar radiation. Two thermoelectric couples were employed as temperature probes to measure the temperature of the inside room.

The  $\text{Cs}_{0.32}\text{WO}_3$  coated fabrics were washed in 0.37% of detergent with 10 steel balls at 30 °C for 45 min in accordance with a standard method AATCC 61–2003 (Colorfastness to Laundering) with some modification, and then rinsed in deionized water three times. Finally, the  $\text{Cs}_{0.32}\text{WO}_3$  coated fabrics were dried at 60 °C. The whole washing process was equivalent to five times of repeated home laundering. The color fastness of the coating on the textile fiber was determined by SEM images.

### III. RESULTS AND DISCUSSION

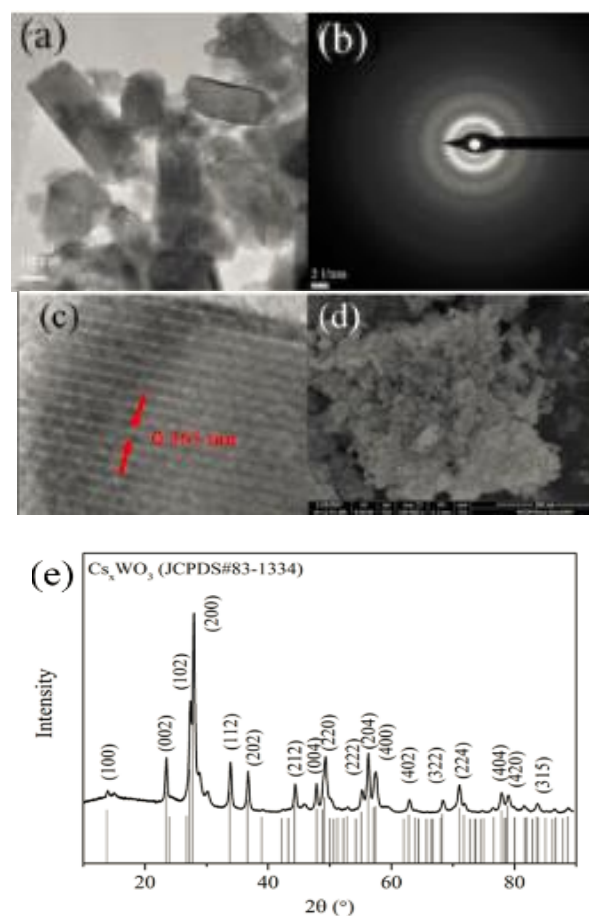
#### A. Morphology and Crystal Structure of $\text{Cs}_{0.32}\text{WO}_3$ Nanosheets

The SEM, TEM, HR-TEM images and diffraction patterns of the  $\text{Cs}_{0.32}\text{WO}_3$  nanosheets are all displayed in Fig. 2. The morphology and size of the as-prepared samples were observed clearly by SEM and TEM. As shown in Fig. 2 (a), the  $\text{Cs}_{0.32}\text{WO}_3$  nanosheets are rectangle thin sheets with a width of 20–30 nm, length up to 50–80 nm.  $\text{Cs}_{0.32}\text{WO}_3$  nanosheets show smooth and clear edges with amorphous impurities. The clear diffraction ring pattern shown in Fig. 2(b) indicates that the  $\text{Cs}_{0.32}\text{WO}_3$  nanosheets are polycrystallines with good crystallinity. Fig. 2(c) shows HRTEM image of  $\text{Cs}_{0.32}\text{WO}_3$  nanosheet, which allows the direct imaging of  $\text{Cs}_{0.32}\text{WO}_3$  nanosheets atomic structure. In this image, it can be seen that  $\text{Cs}_{0.32}\text{WO}_3$  nanosheets are single-crystalline with spacing between lattice fringes of approximately 0.365 nm. This calculated distance between the lattice fringes agreed well with the inter-planar spacing (100) direction of  $\text{Cs}_{0.32}\text{WO}_3$  nanosheet crystal. Fig. 2(d) present the SEM image of  $\text{Cs}_{0.32}\text{WO}_3$  nanosheets are even and uniform in the same size. However,  $\text{Cs}_{0.32}\text{WO}_3$  nanosheets tend to aggregate because there is no driving force on the surface of the nanoparticles to keep them apart.

Fig. 2 (e) shows XRD patterns of  $\text{Cs}_{0.32}\text{WO}_3$  nanosheets. A strong characteristic peak at  $2\theta$  of 27.9 ° is attributed to the crystal face of (200) plane of  $\text{Cs}_{0.32}\text{WO}_3$ . Weak characteristic peaks at  $2\theta$  of 23.4°, 33.8° and 36.6° are assigned to the (002), (112) and (202) reflection lines of  $\text{Cs}_{0.32}\text{WO}_3$ , respectively. The XRD patterns identified by the JCPDS card (file No 83–1334) reveal that the  $\text{Cs}_{0.32}\text{WO}_3$  nanosheets are polycrystalline with a characteristic square crystal structure without any unwanted phase formation. EDS analysis is shown in Fig. 2(f), C is attributed to the carbon tape.  $\text{Cs}_{0.32}\text{WO}_3$  nanosheets contain elements of Tungsten (W), oxygen (O) and cesium (Cs). The atomic ratios of Cs/W is 0.43, which is a little higher than the theoretical value of 0.32. This maybe because EDS is semi-quantitative characterization and some  $\text{Cs}_2\text{CO}_3$  remained in

the samples. However, the results can still confirm that cesium was successfully doped in  $\text{WO}_3$  structure.

IR spectrum of  $\text{Cs}_{0.32}\text{WO}_3$  nanosheets is shown in Fig. 2 (g). In the 5–10  $\mu\text{m}$  and 15–25  $\mu\text{m}$  regions, the IR transmittance is low, which means  $\text{Cs}_{0.32}\text{WO}_3$  nanosheets can block the NIR and FIR transmission. Interestingly, in the 10–15  $\mu\text{m}$  region, which is human body infrared emission range, the IR transmittance of  $\text{Cs}_{0.32}\text{WO}_3$  nanosheets is much higher. It allows the IR emits from the human body can be transferred to the environment rather than be surpassed in the air gap between clothing and the human body. An illustration shown as Fig. 2(h) can further explain the function of the  $\text{Cs}_{0.32}\text{WO}_3$  nanosheets coated cotton fabric. The  $\text{Cs}_{0.32}\text{WO}_3$  nanosheets that coated cotton fabric absorbs the NIR radiation from the sun and convert it into FIR emission to minimize the NIR contact with skins and temperature of air gap between human body and clothing increase. On the other hand, the far IR emits from clothing can enhance blood circulation and metabolism as well as promotes the recovery of fatigued muscles for therapeutic and health care purposes. In addition, the  $\text{Cs}_{0.32}\text{WO}_3$  nanosheets coated fabric shows high transmittance to IR that emits from human body at wavelength of 5–10  $\mu\text{m}$ . This means that the coated fabric facilitates thermal radiation to release to the environment. Therefore, the  $\text{Cs}_{0.32}\text{WO}_3$  nanosheets coated fabric could possess NIR shielding property, FIR emission for health care and high FIR transmittance for heat release at the same time. This multifunctional fabric can be achieved by using single material--  $\text{Cs}_{0.32}\text{WO}_3$  nanosheets.



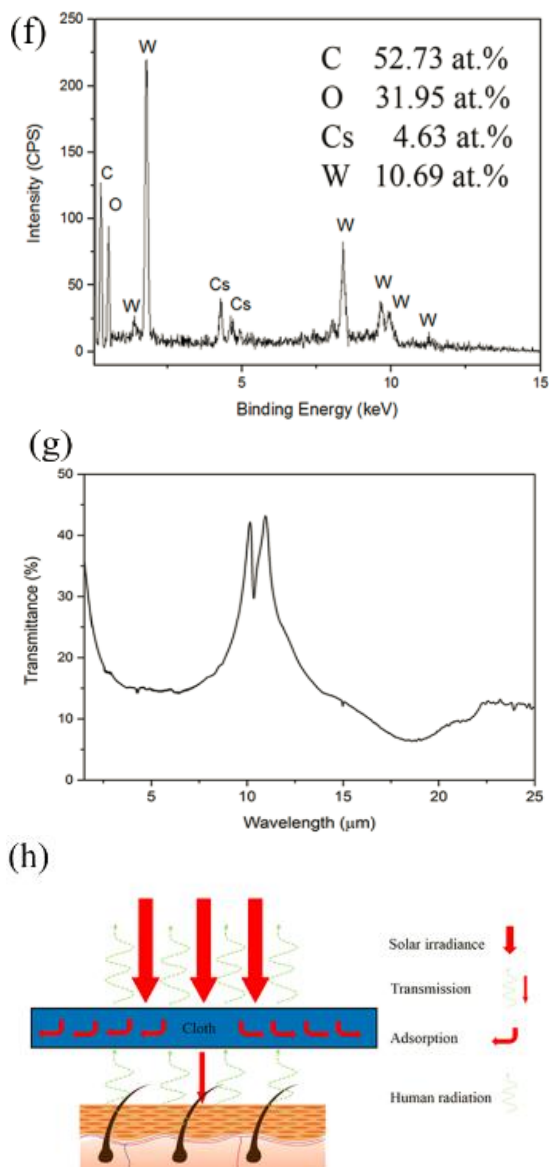


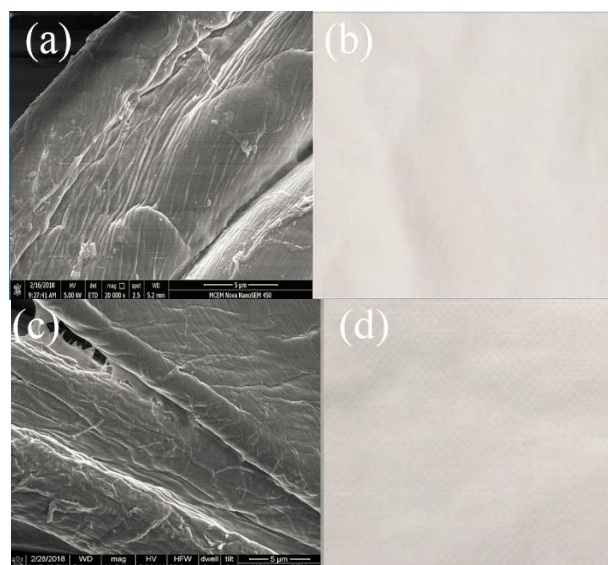
Fig. 2. Characterization of synthesized  $\text{Cs}_{0.32}\text{WO}_3$  nanosheets: (a) TEM image, (b) diffraction ring pattern, (c) high resolution TEM image and (d) SEM image of  $\text{Cs}_{0.32}\text{WO}_3$ , (e) XRD pattern, (f) EDS spectrum, and (g) IR spectrum of  $\text{Cs}_{0.32}\text{WO}_3$  nanosheets, and (h) illustration of NIR absorption of  $\text{Cs}_{0.32}\text{WO}_3$  nanosheets coated cotton fabric.

### B. Surface Morphology of $\text{Cs}_{0.32}\text{WO}_3$ Coated Cotton

Surface morphology of the original and  $\text{Cs}_{0.32}\text{WO}_3$  nanosheets coated cotton fibers were observed by SEM as presented in Fig. 3. It can be seen that the surface of original cotton fibers is rough with some small grooves in Fig. 3(a). A few granules are observed on the surface of cotton fibers due to impurities such as hemicelluloses, lignin, waxes and oils. The appearance of the original cotton is white (Fig. 3 (b)). Fig. 3 (c) shows PDDA treated cotton fiber. A thin film was formed on the surface of the fiber, which can be clearly observed from gaps between fibers. A thin film bridges between the fibers can be observed from SEM image. The surface of the cotton fiber becomes rougher and wrinkled, which means PDDA was successfully coated on the surface of the fiber. In addition, PDDA is colorless (PDDA treated cotton is still in white color) and it doesn't influence the color of the fabric as shown in Fig. 3(d). The purpose of pretreatment of PDDA is to facilitate deposition of  $\text{Cs}_{0.32}\text{WO}_3$  nanosheets on the fiber. This is because cotton

fibers carry negative charges in the neutral solution due to full with hydroxyl groups as well as the  $\text{Cs}_{0.32}\text{WO}_3$  nanosheets. The electrostatic repulsion between  $\text{Cs}_{0.32}\text{WO}_3$  nanosheets and cotton fibers makes it difficult for dense deposition and good adhesion. However, after being treated with PDDA, which is a kind of polymer that carries positive charges, the surface of the cotton fiber is covered with a thin PDDA film. The surface of the cotton fiber carries positive charges after PDDA modification, which is benefit for deposition of negative charged  $\text{Cs}_{0.32}\text{WO}_3$  nanosheets due to the electrostatic attraction. As shown in Fig. 3(e), it can be seen from SEM image that  $\text{Cs}_{0.32}\text{WO}_3$  nanosheets are densely coated on the surface of the cotton fiber. Almost the surface of cotton fibers was fully covered by  $\text{Cs}_{0.32}\text{WO}_3$  nanosheets, which is better for NIR shielding properties. The color of the cotton fabric changes from white to blue (Fig. 3(f)), which comes from  $\text{Cs}_{0.32}\text{WO}_3$  nanosheets. The deeper the color is, the more  $\text{Cs}_{0.32}\text{WO}_3$  nanosheets are coated [16].

Washing fastness is very important for the coating on the textile. It can be seen from Fig. 3(g) and (h), the surface of the cotton fiber is still densely covered by  $\text{Cs}_{0.32}\text{WO}_3$  nanosheets after washing in accordance with AATCC 61. Even the loose  $\text{Cs}_{0.32}\text{WO}_3$  nanosheet aggregations are washed away due to vigorous washing procedures, this small amount of  $\text{Cs}_{0.32}\text{WO}_3$  nanosheets didn't influence the color and performance of the  $\text{Cs}_{0.32}\text{WO}_3$  nanosheets coated fabric, which will be discussed in the following part. This can be explained by that electrostatic attraction between the fibers and aggregations is not strong enough to overcome gravity of big aggregation and friction between steel balls and fibers. The  $\text{Cs}_{0.32}\text{WO}_3$  nanosheets aggregation floated over, while the  $\text{Cs}_{0.32}\text{WO}_3$  nanosheets thin film on the fiber surface. The small size  $\text{Cs}_{0.32}\text{WO}_3$  nanosheets adsorbed on the surface of the fiber show better adhesion strength due to large surface area contact. The appearance of the  $\text{Cs}_{0.32}\text{WO}_3$  nanosheets coated fabric after washing is almost same with the unwashed one (The color of washed  $\text{Cs}_{0.32}\text{WO}_3$  nanosheets coated fabric remains blue as unwashed). The SEM and digital images show that the  $\text{Cs}_{0.32}\text{WO}_3$  nanosheets coated fabric with pretreatment of PDDA shows good washing fastness.



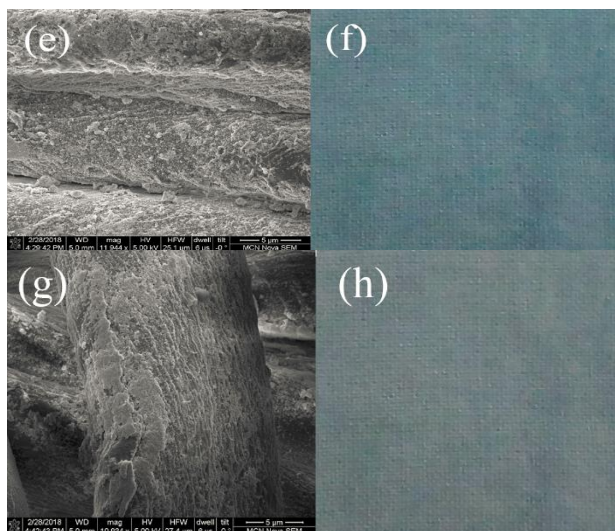


Fig. 3. (a) SEM and (b) digital images of original cotton; (c) SEM and (d) digital images of PDDA treated cotton, (e) SEM and (f) digital images of  $Cs_{0.32}WO_3$  coated cotton and (g) SEM and (h) digital images of  $Cs_{0.32}WO_3$  coated cotton fabric after washing.

### C. ATR IR Spectra and Surface Topography of $Cs_{0.32}WO_3$ Coated Cotton

ATR IR spectra of original, PDDA treated and  $Cs_{0.32}WO_3$  nanosheets coated cotton are shown in Fig. 4(a). The spectra show less difference in these three samples. The characteristic peaks are all attributed to cellulose. The characteristic peaks from PDDA and  $Cs_{0.32}WO_3$  nanosheets are not observed in the spectra because the amount of PDDA is less. The  $Cs_{0.32}WO_3$  nanosheets show no peaks as shown in Fig.2(g). The IR spectra show that the PDDA is in a low amount that didn't influence the chemical structure of cotton.

Atomic force microscopy (AFM) was used to characterize the surface topography of  $Cs_{0.32}WO_3$  nanosheets coated cotton fibers with treatment of PDDA. Fig. 4 (b) and (c) show the AFM 2D and 3D high sensor representations of  $Cs_{0.32}WO_3$  nanosheets coated cotton fibers, respectively. The 2D and 3D images show that the surface of the cotton fiber is rough with some particles coated on the rough surface. The surface roughness increases not obviously due to nanoscale of coating and shape of  $Cs_{0.32}WO_3$  is nanosheet with thin thickness. The original surface of the cotton fiber shows microscale roughness in SEM images, while the nanoscale roughness of  $Cs_{0.32}WO_3$  nanosheets coated fabric increased after coating. To further investigate the surface topography of coated fiber, the average surface roughness of the five selected cross-section lines on the fiber was calculated by the software. The average calculated value of roughness (Ra) obtained for  $Cs_{0.32}WO_3$  nanosheets coated cotton fibers is 12.68 nm. The results confirm that the  $Cs_{0.32}WO_3$  nanosheets coating doesn't cause much surface roughness increasing due to small size and thin thickness of  $Cs_{0.32}WO_3$  nanosheets. The irregular round shape of  $Cs_{0.32}WO_3$  nanosheets was causing by the deviation in the plane image resulting from the broadening effect of the AFM tip. The height sensor results are accurate. The relatively smooth surface after coating is also benefit for washing fastness. Actually, shape of  $Cs_{0.32}WO_3$  nanosheets is rectangle sheets with large surface area around  $58 \text{ m}^2/\text{g}$ . Large surface area of  $Cs_{0.32}WO_3$

nanosheets contacts with cotton fiber so that they are adhered on the surface of the fiber firmly. The AFM results confirm the  $Cs_{0.32}WO_3$  nanosheets densely coating on the surface of cotton fiber and not causing much surface roughness increasing.

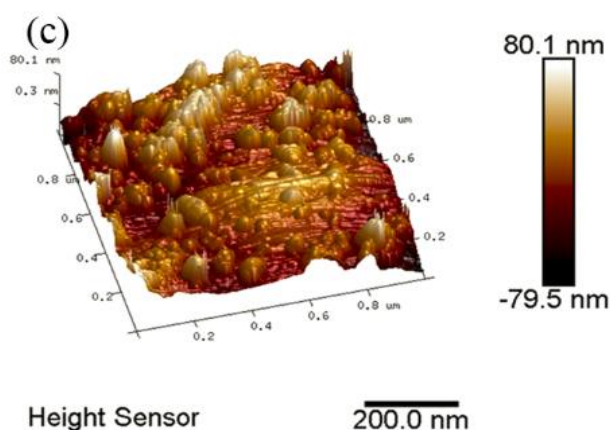
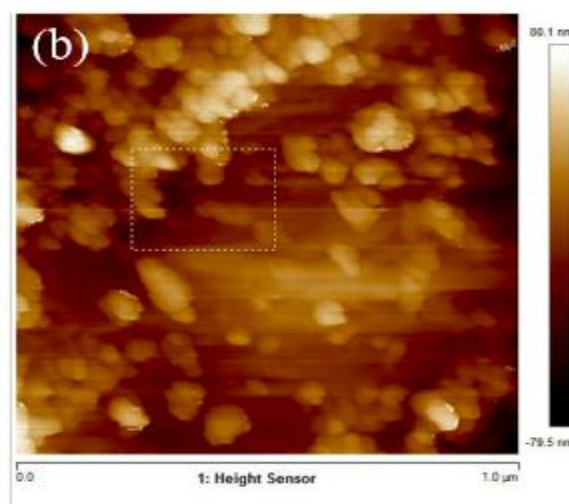
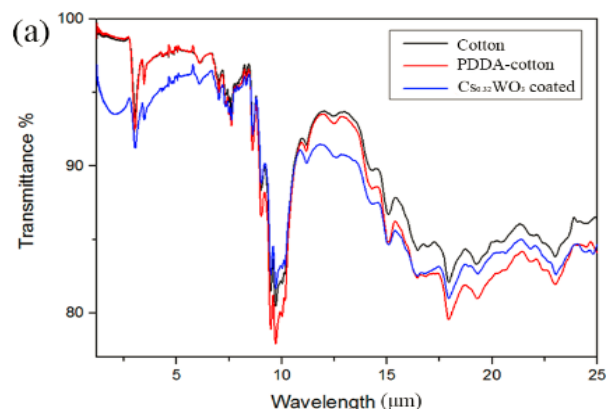


Fig. 4. (a) ATR IR spectra and AFM (b) 2D and (c) 3D images of  $Cs_{0.32}WO_3$  nanosheets coated fabric.

### D. Near Infrared Shielding and Far Infrared Emission Properties of $Cs_{0.32}WO_3$ Nanosheets Coated Cotton Fabric

A simulation test was conducted to study the NIR shielding property of  $Cs_{0.32}WO_3$  coated fabric. The infrared lamp simulates the solar radiation and an insulated box with a window on top simulates the environment under sample. The window was covered by original fabric and  $Cs_{0.32}WO_3$  nanosheets coated one to compare the NIR shielding

property of  $\text{Cs}_{0.32}\text{WO}_3$  coated fabric with the original one (as shown in Fig.5 (b)).

The surface temperature of  $\text{Cs}_{0.32}\text{WO}_3$  nanosheets coated fabric is shown in top of Fig. 5(a). The surface temperature of the original cotton fabric and  $\text{Cs}_{0.32}\text{WO}_3$  nanosheets coated fabric increased from 27 °C to 33.7 °C and 64.0 °C within 5 min after radiation, respectively. Then a thermal equilibrium is reached. The surface temperature of samples were recorded by IR camera as shown in Fig. 5(c). IR camera uses color distribution to show the temperature distribution on the surface. The whiter the color is, the higher the temperature is. The IR images on the right side confirms the temperature increase of the  $\text{Cs}_{0.32}\text{WO}_3$  coated fabric. The temperature of yellow-white area is much higher than that of purple area. The surface temperature of original cotton and PDDA treated cotton is 33.7 °C, which is much lower than that of  $\text{Cs}_{0.32}\text{WO}_3$  coated fabric (64.0 °C) after 20 min radiation. This phenomenon suggests that  $\text{Cs}_{0.32}\text{WO}_3$  nanosheets adsorb large amount of NIR, and then increase their own temperature to transfer it into FIR, while original cotton fabric allows NIR transfer to human skin. The results show that the  $\text{Cs}_{0.32}\text{WO}_3$  coated fabric possess excellent NIR shielding and FIR emission properties (The temperature of  $\text{Cs}_{0.32}\text{WO}_3$  coated fabric increases to 64.0 °C). The phenomenon can be explained by that cotton fabric is regarded as a black body. The IR radiation is emitted by matters (the temperature is higher than absolute zero) according to Planck's law. This means that it has a spectrum that is determined by the temperature alone, not by the body's shape or composition. Therefore, the  $\text{Cs}_{0.32}\text{WO}_3$  coated fabric emits far infrared with wavelength ranging from 5 $\mu\text{m}$  to 100 $\mu\text{m}$  at this temperature, which is benefit to human body without much thermal effect.

Two model houses were used to demonstrate the IR shielding property of  $\text{Cs}_{0.32}\text{WO}_3$  coated fabric as shown in Fig. 5(d). The inside temperatures of the both two model houses are 12.3 °C before simulated solar radiation. Two lamps were set up in front of the model houses. After 5 min irradiation, temperature-difference between the inner-rooms with  $\text{Cs}_{0.32}\text{WO}_3$  coated fabric and uncoated fabric was significant ( $\text{Cs}_{0.32}\text{WO}_3$  coated fabric is 4.5 °C lower than original one), which suggested that a significant amount of irradiation was blocked by the  $\text{Cs}_{0.32}\text{WO}_3$  coated fabric. This result also confirms that  $\text{Cs}_{0.32}\text{WO}_3$  coated fabrics have excellent thermoregulation effects.

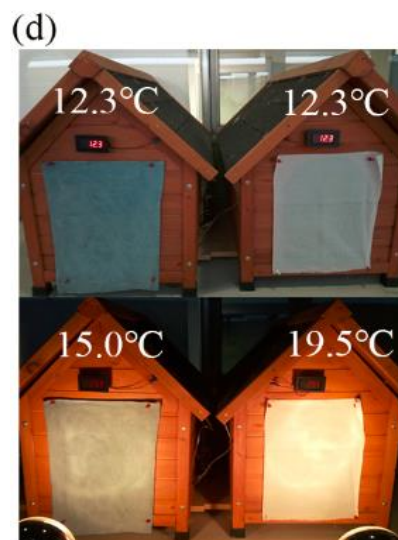
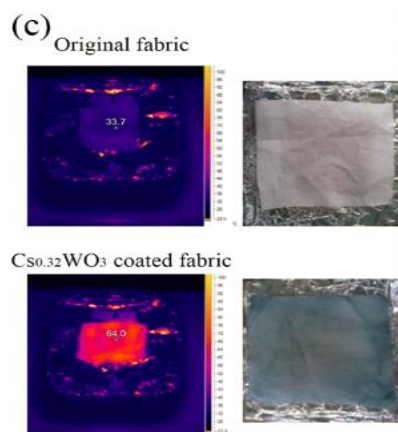
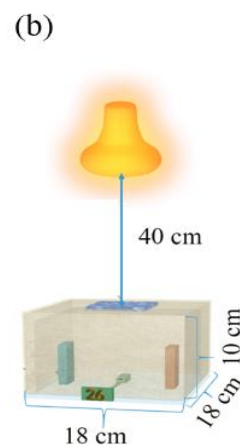
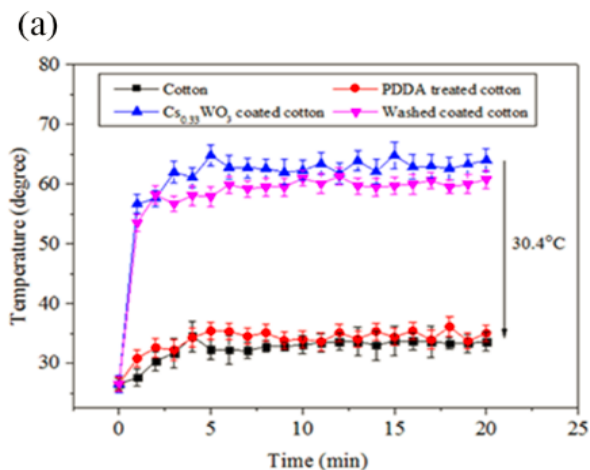


Fig.5. NIR shielding property and FIR emission of  $\text{Cs}_{0.32}\text{WO}_3$  coated fabric: (a) temperature of the samples surface, (b) illustration of simulation test device, (c) IR and digital images of the surface temperature of original and  $\text{Cs}_{0.32}\text{WO}_3$  coated fabrics, and (d) model house demonstration of before and after 5 min simulated solar radiation.

#### IV. CONCLUSION

In this study,  $\text{Cs}_{0.32}\text{WO}_3$  nanosheets were synthesized through ball milling process, which is waterless and environmental friendly.  $\text{Cs}_{0.32}\text{WO}_3$  nanosheets were self-assembled on the surface of cotton with treatment of PDDA for NIR shielding and FIR emission purposes. The surface morphology, crystal structure, NIR shielding and FIR emission of  $\text{Cs}_{0.32}\text{WO}_3$  coated cotton fabrics were investigated. The results shows the  $\text{Cs}_{0.32}\text{WO}_3$  nanosheets

are rectangle nanosheets with thin thickness and good crystalline.  $\text{Cs}_{0.32}\text{WO}_3$  nanosheets are evenly and firmly coated onto the cotton fabrics treated with PDDA and the as-prepared samples show very good NIR shielding property of lowering the inner-rooms temperature of 4.5 °C and washing durability were comprehensively maintained. In addition,  $\text{Cs}_{0.32}\text{WO}_3$  coated cotton fabric converts NIR into FIR to decrease the thermal transfer towards the skin. This kind of NIR shielding and FIR emission fabric shows great potential applications in physical therapy area, household textiles, outdoor textiles and so on. The large scale fabrication of  $\text{Cs}_{0.32}\text{WO}_3$  nanosheets and coated textiles can be achieved by ball-milling and self-assembly methods, respectively, even though they are a little time consuming.

#### CONFLICT OF INTEREST

The authors declare no conflict of interest.

#### AUTHOR CONTRIBUTIONS

Linghui Peng conducted the research; Weifan Chen analyzed the data; Linghui Peng wrote the paper; all authors had approved the final version.

#### ACKNOWLEDGMENT

We gratefully acknowledge the financial support of the National Natural Science Foundation of China (Project Nos.21761020 and 51464033), China Scholarship Council, access to Melbourne Centre of Nanofabrication (MCN), Monash Centre for Electronic Microscopy (MCEM), and the Australian Research Council (ARC) (Project Nos.DP160104456 and FT0990942).

#### REFERENCES

- [1] N. A. Staylor, "Challenges to temperature regulation when working in hot environments," *Industrial Health*, vol. 44, pp. 331-344, 2006.
- [2] F. R. de Grujil, H. J. van Kranen, and L. H. Mullenders, "UV-induced DNA damage, repair, mutations and oncogenic pathways in skin cancer," *J. Photochem. Photobiol., B*, vol. 63, pp. 19-27, 2001.
- [3] B. A. Çakır, L. Budama, Ö. Topel, and N. Hoda, "Synthesis of ZnO nanoparticles using PS-b-PAA reverse micelle cores for UV protective, self-cleaning and antibacterial textile applications," *Colloids Surf. A*, vol. 414, pp. 132-139, 2012.
- [4] L. H. Peng, R. H. Guo, J. W. Lan, S. W. Jiang, and X. Wang, "Silver nanoparticle coating on cotton fabric modified with poly (diallyldimethylammonium chloride)," *Mater. Technol.*, vol. 31, pp. 431-436, 2015.
- [5] J. Tian, Y. Leng, Z. H. Zhao, Y. Xia, Y. H. Sang, P. Hao, J. Zhan, M. C. Li, and H. Liu, "Carbon quantum dots/hydrogenated  $\text{TiO}_2$  nanobelt heterostructures and their broad spectrum photocatalytic properties under UV, visible, and near-infrared irradiation," *Nano Energy*, vol. 11, pp. 419-427, 2015.
- [6] C. L. Zhang, C. Zhang, R. Huang, and X. Y. Gu, "Effects of hollow microspheres on the thermal insulation of polysiloxane foam," *J. Appl. Polym. Sci.*, vol. 134, January 2017.
- [7] C. Wang, C. Xiang, L. Tan, J. Wang, L. Peng, S. Jiang, and R. Guo, "Preparation of silver/reduced graphene oxide coated polyester fabric for electromagnetic interference shielding," *RSC Advances*, vol. 7, pp. 40452-40461, 2017.
- [8] K. Panwar, M. Jassal, and A. K. Agrawal, " $\text{TiO}_2$ - $\text{SiO}_2$  Janus particles treated cotton fabric for thermal regulation," *Surf. Coat. Technol.*, vol. 309, pp. 897-903, 2017.
- [9] A. J. Fitzgerald, E. Berry, N. N. Zinovev, G. C. Walker, M. A. Smith and J. M. Chamberlain, "An introduction to medical imaging with coherent terahertz frequency radiation," *Phys. Med. Biol.*, vol. 47, p. 67, 2002.

- [10] C. H. Park, M. H. Shim, and H. S. Shim, "Far IR emission and thermal properties of ceramics coated fabrics by IR thermography," *Key Eng. Mater.*, vol. 321, pp. 849-852, 2006.
- [11] X. Hu, M. Tian, L. Qu, S. Zhu, and G. Han, "Multifunctional cotton fabrics with graphene/polyurethane coatings with far-infrared emission, electrical conductivity, and ultraviolet-blocking properties," *Carbon*, vol. 95, pp. 625-633, 2015.
- [12] S. Inoue and M. Kabaya, "Biological activities caused by far-infrared radiation," *Int. J. Biometeorol.*, vol. 33, pp. 145-150, 1989.
- [13] K. Washington, J. Wason, M. S. Thein, L. A. Lavery, M. R. Hamblin, and I. L. Gordon, "Randomized controlled trial comparing the effects of far-infrared emitting ceramic fabric shirts and control polyester shirts on transcutaneous  $\text{PO}_2$ ," *J. Text. Sci. Eng.*, vol. 8, pp. 1-17, 2018.
- [14] H. Ono, "Far infrared radiation health appliance and method of use," U.S. Patent, no. 6549, p. 809, April 2003.
- [15] Z. Yu, Y. Yao, J. Yao, L. Zhang, Z. Chen, Y. Gao, and H. Luo, "Transparent wood containing  $\text{Cs}_x\text{WO}_3$  nanoparticles for heat-shielding window applications," *J. Mater. Chem. A*, vol. 5, pp. 6019-6024, 2017.
- [16] L. Peng, W. Chen, B. Su, A. Yu, and X. Jiang, "Cs<sub>x</sub>WO<sub>3</sub> nanosheet-coated cotton fabric with multiple functions: UV/NIR shielding and full-spectrum-responsive self-cleaning," *Appl. Surf. Sci.*, vol. 475, pp. 325-333, December 2019.
- [17] X. Fang, M. Yao, L. Guo, Y. Xu, W. Zhou, M. Zhou, C. Shi, L. Liu, L. Wang, X. Li, and W. Chen, "One-step, solventless, and scalable mechanosynthesis of  $\text{WO}_3 \cdot 2\text{H}_2\text{O}$  ultrathin narrow nanosheets with superior UV-vis-light-driven photocatalytic activity," *ACS Sustainable Chem. Eng.*, vol. 5, pp. 10735-10743, May 2017.

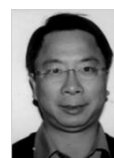
Copyright © 2019 by the authors. This is an open access article distributed under the Creative Commons Attribution License which permits unrestricted use, distribution, and reproduction in any medium, provided the original work is properly cited ([CC BY 4.0](https://creativecommons.org/licenses/by/4.0/)).



**Linghui Peng** is a PhD student of Department of Chemical Engineering, Monash University (Australia). She received her B.E. degree in textile engineering (2014) and B.B.A degree in business administration (2014), and M.E. degree in textile chemistry and dyeing and finishing engineering (2017) from Sichuan University (China). She worked as a research assistant during 2016-2017 at the Hong Kong Polytechnic University. She then held the CSC (Chinese Scholarship Council) scholarship to study in Monash University (2017 to present). Her current scientific interest is focused on synthesis of metal oxides nanoparticles for energy saving applications including thermal management and self-cleaning textiles and glasses.



**Weifan Chen** is a professor in the School of Materials Science and Engineering, Nanchang University. He is a researcher in rare earth and micro nano functional materials research center of Nanchang University. He worked in a technological company for technology development for more than ten years. He obtained the PhD. from Nanjing University of Science and Technology in Jan 2001 and joined Nanchang University in April 2007. He visited professor Aibing Yu's group in Monash University from September 2017 to September 2018.



**Aibing Yu** is vice chancellor's professorial fellow, pro vice-chancellor and president of Monash-SEU Joint Research Institute, and director, Australia-China Joint Research Centre on minerals, metallurgy and Materials. He obtained the B.Eng. in 1982 and the M.Eng. in 1985 from Northeastern University (China), and the Ph.D. in 1990 from the University of Wollongong (Australia). His research is mainly in particle science and technology, and process and materials engineering. He is an elected fellow of the Australian Academy of Technological Sciences and Engineering, and Australian Academy of Science.



**Xuchuan Jiang** is in the Department of Chemical Engineering at Monash University. He is devoted to the study of synthesis, self-assembly, and applications of functional nanoparticles since the award of his Ph.D. in 2001. He has worked in various academic research institutes, including University of Washington (USA), University of Paris (France), University of New South Wales (Australia) and Monash University (Australia). He was awarded an Australia Research Council (ARC) future fellowship in 2009.